E 121H

FERMILAB-PUB-76-127-E

UCD PPL 76-11-01

Extraction of Average Multiplicity of high energy off-mass-shell $\pi\pi$ and $K\pi$ Scattering.*

J. Erwin, R.D. Kass, J.H. Klems, Winston Ko, R.L. Lander,

D.E. Pellett and P.M. Yager

Department of Physics

University of California

Davis, CA 95616

and

M. Alston-Garnjost

Lawrence Berkeley Laboratory

University of California

Berkeley, CA 94720

* Work supported in part by the U.S. Energy Research and Development Administration.

Abstract

Inclusive $\Delta^{++}(1236)$ and Λ° production in $\pi^{+}p$ and pp interactions is examined in terms of a one meson exchange model. We find inclusive Δ^{++} production to be consistent with one pion exchange, and if one demands a gap of at least one unit of rapidity between the Λ° and its recoiling mass, inclusive Λ° production is consistent with one kaon exchange. The average charge multiplicity, $\langle N_{CH} \rangle$, recoiling from the Δ^{++} and Λ° is studied as a function of massing mass M^2 for both $\pi^{+}p$ and pp interactions.

Introduction

There has been increasing evidence[1-5] that inclusive $\Delta^{++}(1236)$ production in the hundred GeV range is mediated by one pion exchange. In this paper we show that this is also the case for both the pp and π^+p interactions at 100 GeV/c. The average multiplicity, $< N_{CH} >$, of the mass recoiling off the Δ^{++} produced in pp interactions is shown to be consistent with that of π^-p scattering. Examining the mass recoiling against the Δ^{++} from π^+p interactions allows us to study $< N_{CH} >$ for off-mass-shell $\pi^-\pi^+$ interactions.

The quantum numbers for a $\Lambda°$ produced backward in the center of mass off a proton target are consistent with kaon exchange. Analysis of the mass recoiling against the $\Lambda°$ for the reaction $\pi^+p \rightarrow \Lambda°X$ allows us to study $< N_{CH} >$ for off-mass-shell $K^+\pi^+$ scattering. A consistency check of $< N_{CH} >$ is obtained by extracting $< N_{CH} >$ for off-mass-shell K^+p from the process $pp \rightarrow \Lambda°X$ at 100 GeV and comparing it with the on-mass-shell values.

Scanning and Measurement

The data consist of an approximately 100,000 picture exposure of the Fermi National Accelerator Laboratory's 30 inch hydrogen bubble chamber to a mixed, tagged positive beam at 100 GeV/c.[6] This exposure yielded

7821 pp events, 4304 π^+p events and a combined total of 2418 events with at least one neutral strange particle decay or γ conversion. The tracks from the primary vertex were measured twice on a Lawrence Berkeley Laboratory spiral reader.[7] Half of the neutral decays and conversions were measured on a LBL Franckenstein, the other half were measured on a spiral reader.[8] All remeasurements were made on a Franckenstein. The measurements were processed using the programs POOH and TVGP. The program SQUAW was used to fit the neutral decays and conversions that were unambiguously identified with a primary vertex and also to fit the 4 constraint hypothesis for events with no V's. The overall scanning efficiency for V's was 96%, while the overall measurement efficiency for neutral decays and conversions was 89%. The scanning efficiency for four prongs and higher multiplicities was 99%, and for two prongs was 93%.

The efficiency for measuring positive tracks in the backward hemisphere in the C.M. system is about 96% for all topologies. Thus we have a high efficiency for measuring the two positive tracks decaying from a slow Δ^{++}. Protons were distinguished from pions or kaons both by automatic ionization information and by a visual check of bubble density for laboratory momentum up to 1.3 GeV/c.

Tracks from neutral decays were assigned an identity, when possible, by using ionization information. Ambiguous events were selected on the basis of the confidence level of the kinematic fit and the transverse momentum of the decay tracks with respect to the line of flight of the neutral. Strange particle decays were rejected if they were within 2 cm of the production vertex. The number of decays satisfying the criteria of a Λ° were 135 (57) for pp (π^+p) interactions. The contamination of the Λ° by γ's is estimated to be less than 5%.

Inclusive $\Delta^{++}(1236)$ Production

Since we can distinguish protons from mesons for laboratory momentum up to 1.3 GeV/c, a cut of $|t_{p\Delta^{++}}| < .88$ GeV^2 is imposed in order to insure that all decay angles of the Δ^{++} are covered. The invariant mass of all proton - π^+ combinations with $|t_{p\Delta^{++}}| < .88$ GeV^2 is shown in Figure 1. A strong $\Delta^{++}(1236)$ signal is seen for both pion and proton induced events. After imposing the above mentioned $|t|$ cut and correcting for background, the inclusive production cross sections of Δ^{++} produced in the backward hemisphere are 1.24 $\pm$ .12 and 1.04 $\pm$ 0.10 mb for pp and π^+p interactions.[9] The pp result is in agreement with the result of Ref. 3, 1.36 $\pm$ .14 mb. For the rest of this paper a Δ^{++} is defined to be any proton-π^+ combination with $1.16 \leq m(\pi^+p) \leq 1.32$ GeV and is limited to $|t| < .88$ GeV^2. For those cases (24 events for pp, 22 events for π^+p) where more than one π^+p combination satisfies our selection criteria, we chose the combination which has the mass closest to 1.236 GeV.

To test for one pion exchange we study the spin alignment of the π^+p pair in terms of the Treiman-Yang angle and the Jackson angle. The decay angles of the proton are computed in the rest frame of the Δ^{++}, the t channel frame. In this frame, the z axis is the direction of the target-particle momentum ($\vec{p}$) and the y axis is defined by $\vec{q} \times \vec{p}$, where $\vec{q}$ = momentum of the beam particle. The distribution in the Treiman-Yang angle is shown in Figure 2. For both $pp \to \Delta^{++}X^\circ$ and $\pi^+p \to \Delta^{++}X^\circ$ this distribution is flat,

consistent with one pion exchange. The t channel decay density matrix element $\text{Re}\rho_{3-1}$ is determined to be 0.00 ± 0.03 for $pp \to \Delta^{++}X^\circ$ and $- 0.03 \pm .04$ for $\pi^+p \to \Delta^{++}X^\circ$. These values are in agreement with zero, as expected from one pion exchange. Additional evidence of one pion exchange is provided by the Jackson angle ($\cos\theta$) distribution, also shown in Figure 2. The $\cos\theta$ distributions are found to be consistent with predictions of either the one pion exchange model ($dN/d(\cos\theta) = 1 + \cos^2\theta$) or the one pion exchange absorptive model ($dN/d(\cos\theta) = .37 + .39 \cos^2\theta$). We find (not shown) that for $M(\pi^+p) > 1.32$ GeV the Jackson angle distribution is strongly peaked in the forward ($\cos\theta = 1$) direction. This difference in the distribution is additional evidence that we have a strong Δ^{++} signal. In the Δ^{++} region ρ_{33} is determined to be $0.13 \pm .04$ for both p induced and π^+ induced reactions. Knowing that background is surely present and recalling the big difference between the Jackson angle distributions in the Δ^{++} region and the region of higher π^+p masses, we do not feel that our measurement of ρ_{33} distinguishes between the one pion exchange ($\rho_{33} = 0$) and the one pion exchange absorptive model ($\rho_{33} = .12$). In summary, the spin alignment study here shows that inclusive Δ^{++} production at 100 GeV/c is consistent with one pion exchange in both π^+p and pp interactions.

Off-Mass-Shell π^-p and $\pi^-\pi^+$ Scattering

The diagram in Figure 3a represents inclusive Δ^{++} production via one pion exchange. If, however, one wants to study the inelastic multiplicity of the mass recoiling against the Δ^{++}, events due to processes shown in Figure 3b must be removed (e.g. $N^{*+} \to \Delta^{++}\pi^-$). These events are four prongs that are consistent with no π°'s or neutral strange particles being produced (4C-4Prong).[10] In terms of Figure 3b a 4C-4 Prong event is an event of elastic π^-p or $\pi^-\pi^+$ scattering. Therefore, in order to study the inelastic production of X° via π^- exchange, these 4C-4 Prong events must be removed. Figure 4 shows the square of the recoiling mass of all events and with the 4C-4 Prongs removed.

After removing the 4C-4 Prong events in $pp \rightarrow \Delta^{++}X^\circ$ the multiplicity of X° should agree with that of the known multiplicity of inelastic $\pi^- p$ interactions. We parameterized the on-mass-shell $\pi^- p$ inclusive multiplicity by eq. (1)

$$< N_{CH} > = - 4.5 + 10/\sqrt{s} + 2 \ln s \; . \quad (1)$$

[11]

The left hand side of Figure 5 shows excellent agreement between the average multiplicity of X° from $pp \rightarrow \Delta^{++}X^\circ$ without the 4C-4 Prong events and eq. (1) (compared at the same M^2 as s for the on-mass-shell reactions).

In order to extract the average $\pi^-\pi^+$ inelastic multiplicity (right side of Figure 5) we remove the 4C-4 Prong events from $\pi^+ p \rightarrow \Delta^{++}X^\circ$. The average $\pi^-\pi^+$ inelastic multiplicity that we extract is an average of 0.6 units higher than for $\pi^- p$. Although the $\pi^-\pi^+$ multiplicity appears to be qualitatively flatter than the $\pi^- p$ multiplicity, it is not inconsistent with the same functional form shifted upward. It is well known that the $\pi^+ p$ average multiplicity is higher than the pp average multiplicity by about 0.3 units.[5,11] We have now observed that the $\pi^-\pi^+$ average multiplicity is even higher (by about 0.6 units) than that of $\pi^+ p$ interactions.

Inclusive Λ° Production

The total inclusive cross section for Λ° production is 1.1 ± 0.2 mb for $\pi^+ p \rightarrow \Lambda^\circ X^{++}$ and 3.5 ± 0.4 mb for $pp \rightarrow \Lambda^\circ X^{++}$.[8] To calculate the cross section for $pp \rightarrow \Lambda^\circ X$ the Λ°'s that were going backward in the center of mass and the symmetry of the reaction was used. The cross section for $\pi^+ p \to \Lambda^\circ X^{++}$ uses Λ°'s from both center of mass hemispheres. For the rest of this paper only Λ°'s produced backward in the center of mass are used.

It is interesting to note that in $\pi^+ p$ interactions there are no 2 prong events with a Λ°, and in pp interactions there is only one event of the type $pp \to \Lambda^\circ K^+ p$ (elastic Kp scattering). Figure 6 shows the square of the mass recoiling from the Λ°. This distribution is peaked toward higher M^2 values.

Our large bins in M^2 are not merely due to limited statistics. Even with good statistics, the M^2 distribution will be smeared by an unknown amount of Σ° production. It is reasonable to assume that Λ° and Σ° are produced in the same way, since they would involve exchange of the same quantum numbers. However, the square of the missing mass recoiling from the Λ°, $M^2_{\Lambda^\circ}$, from $\Sigma^\circ \to \Lambda^\circ \gamma$, is not always a good measure of the square of the missing mass from the parent Σ°, $M^2_{\Sigma^\circ}$. In the extreme cases where the γ makes a large angle with the recoiling mass as viewed in the rest system of the Σ°, $M^2_{\Lambda^\circ}$ is an over-estimate of $M^2_{\Sigma^\circ}$. The bounds of M^2 are given in eq. (2):

$$M^2_{\Lambda^\circ} = \frac{1}{2m^2_{\Sigma^\circ}} \left[[m^2_{\Sigma^\circ} + m^2_{\Lambda^\circ}) M^2_{\Sigma^\circ} + (m^2_{\Sigma^\circ} - m^2_{\Lambda^\circ})(s - m^2_{\Sigma^\circ} \pm \lambda^{\frac{1}{2}} (s, M^2_{\Sigma^\circ}, M^2_{\Lambda^\circ}) \right] \tag{2}$$

where: $\lambda(s, M^2_{\Sigma^\circ}, M^2_{\Lambda^\circ}) = (s - (M_{\Sigma^\circ} + M_{\Lambda^\circ})^2\ (s - (M_{\Sigma^\circ} - M_{\Lambda^\circ})^2)$

m_{Σ° = rest mass of Σ°

m_{Λ° = rest mass of Λ° .

For the energy of our experiment, Figure 7 shows the bounds of the uncertainty, $M^2_{\Lambda^\circ} - M^2_{\Sigma^\circ}$, as a function of $M^2_{\Sigma^\circ}$ when the Λ is actually the product of $\Sigma^\circ \to \Lambda^\circ\gamma$. It is not meaningful to have a bin size smaller than the smear. Fortunately the region with the best statistics (large M^2) is also the place where the smearing due to Σ° production is the smallest.

Off-mass-shell K^+p and $K^+\pi^+$ scattering

There is recent evidence [12] that inclusive Λ° production in pp interactions is mediated by kaon exchange. For the reaction $pp \to \Lambda^\circ X^{++}$, $\langle N_{CH}(X^{++}) \rangle$ is, in the kaon exchange picture, the average multiplicity of the off-mass-shell K^+p scattering. The average multiplicity of the X^{++} system as a function of M^2 is shown in Figure 8. We compare these values to the average multiplicity of the on-mass-shell K^+p scattering of $s = M^2$. Relatively few data are available for on-mass-shell K^+p inelastic scattering. We find that eq. (1), which represents the on-mass π^-p inelastic multiplicity, can represent those (K^+p) data with an uncertainty of $\pm$ 0.4 units.

Figure 8 (left side) shows the inelastic multiplicity associated with the Λ in pp interactions compared with eq. (1). Except at very large M^2 the off-mass-shell multiplicity (dashed points) agrees with that for on-mass-shell K^+p and π^-p scattering. As s/M^2 becomes small, so does the rapidity gap, Δy, between the $\Lambda^\circ$and its missing mass. The one particle exchange picture is not expected to be valid when Δy falls below one unit. Demanding a rapidity gap of at least one unit between the Λ° and its missing mass (solid data points), one obtains good agreement with on-mass-shell K^+p and π^-p scattering. With Δy less than 1, Λ°'s are presumably produced in some other process, the average multiplicity of which seems to be higher.

The average multiplicity associated with the Λ° in π^+p interactions is shown in Figure 8 (right side). At large M^2, the solid and dashed points are those with and without at least one unit of rapidity between the Λ° and its missing mass. The solid points are the extracted average multiplicities of $K^+\pi^+$ scattering. The values of the average multiplicities for $K^+\pi^+$ are close to one unit above that of K^+p for all M^2.

Conclusion

We conclude that the effect which we observed in pion exchange from inclusive Δ^{++} production is also present in kaon exchange. The average multiplicity in off-mass-shell meson proton scattering agrees with the on-mass-shell values, and meson-meson scattering has a higher average multiplicity than baryon-meson scattering.

Acknowledgments

We thank the staffs of the 30-inch Bubble Chamber and Neutrino Laboratory of the Fermi National Accelerator Laboratory for their assistance. The aid of the Proportional Hybrid System Consortium is gratefully acknowledged. We also thank the scanning and measuring staffs at the University of California, Davis, and the Lawrence Berkeley Laboratory.

References and Footnotes

1. F.T. DAO, D. GORDON, J.LACH, E. MALAMUD, T. MEYER, R. POSTER, P.E. SCHLEIN, W.E. SLATER, Phys. Rev. Lett. 30, 34(1973).
2. E. GOTSMAN, Phys. Rev. D9, 9(1974).
3. J.P. DeBRION, C. BROMBERG, T. FERBEL, T. JENSEN, R. SCHINDLER, P. SLATTERY, A.A. SEIDL, J.C. VANDER VELDE, Phys. Rev. Lett. 34, 190 (1975).
4. S. BARISH, M. DERRICK, B. MUSGRAVE, P. SCHULTZ, J. WHITMORE, R. ENGELMANN, T. KAFKA, M. PRATAP, Phys. Rev. D5, 1260(1975).
5. J. ERWIN, R.D. KASS, J.H. KLEMS, WINSTON KO, R.L. LANDER, D.E. PELLETT, P.M. YAGER and M. ALSTON-GARNJOST, Phys. Rev. Lett. 35, 980(1975).
6. J. ERWIN, J.H. KLEMS, W. KO, R.L. LANDER, D.E. PELLETT, P.M. YAGER and M. ALSTON-GARNJOST, Phys. Rev. Lett. 32, 254(1974).
7. J. ERWIN, W. KO, R.L. LANDER, D.E. PELLETT, P.M. YAGER, M. ALSTON-GARNJOST, Phys. Rev. Lett. 33, 1352(1974).
8. Margaret ALSTON-GARNJOST, J. ERWIN, J.H. KLEMS, W. KO, R.L. LANDER, D.E. PELLETT and P.M. YAGER, Phys. Rev. Lett. 35, 142(1975).
9. The background under the Δ^{++} signal was estimated to be 36% for pp and 31% for π^+p events.
10. D. BRICK, B. HABER, M. HODOUS, R. HULSIZER, V. KISTIAKOWSKY, A. LEVY, A. NAKKASYAN, I. PLESS, V. SIMAK, P. TREPAGNIER, J. WOLFSON, R. YAMAMOTO; Phys. Rev. Lett. 31, 488(1973).

11. J. WHITMORE, Physics Reports 10C (1974). The curve shown in Fig. 6 is from Tow, Phys. Rev. D7, 3535(1973), parameterized $< N_{CH} >$ to $a + b/\sqrt{s} + c \ln s$. We normalized the curve to fit the $\pi^- p$ data with $a = -4.5$, $b = 10$ and $c = 2$.

12. K. ALPGÅRD et al., Nuclear Physics B105, 349(1976).

Figure Captions

Fig. 1 Invariant mass $m(\pi^+p)$ for all πp combinations. There is a $|t_{p\to\pi^+p}|$ cut of 0.88 GeV^2 made on the data. The above figure corresponds to 809 (711) weighted pp (π^+p) events.

Fig. 2 The t-channel decay angles of the Δ^{++}. The ϕ distributions are compared with a normalized constant. The $\cos\theta$ distributions are compared with both the one-pion-exchange ($1+3\cos^2\theta$ in solid line) and one-pion-exchange with absorbtion ($0.37 \pm 0.39\cos^2\theta$ in dotted line).

Fig. 3 (a) One-pion-exchange diagram representing the production process of Δ^{++}.

(b) Diagram for Δ^{++} production in 4c 4-prong events. To isolate off-mass-shell π^- inelastic scattering we remove events represented by diagram 3b.

Fig. 4 Distribution of recoiling mass square M^2 of the X°. The shaded distributions do not include 4c 4-prong events. See Footnote 9 for background.

Fig. 5 The average charge multiplicity of X° as function of M^2, not including 4c 4-prongs. The curve shown is a fit of the π^-p on-mass-shell inelastic charge multiplicity with substitution of $M^2 = s$. (Ref. 11).

Fig. 6 Distribution of the square of the mass recoiling off the Λ.

Fig. 7 For Λ's as product of $\Sigma^0 \rightarrow \Lambda\gamma$, the bounds of the over-estimate of M_Σ^2 when M_Λ^2 is used.

Fig. 8 The average charge multiplicity of X^{++} versus M^2. At large M^2, the solid and dashed points are those with and without demanding at least one unit of rapidity gap between the Λ and its missing mass. The curve represents the average multiplicity in on-mass-shell K^+p scattering (same as π^-p scattering), with the substitution $M^2 = s$.

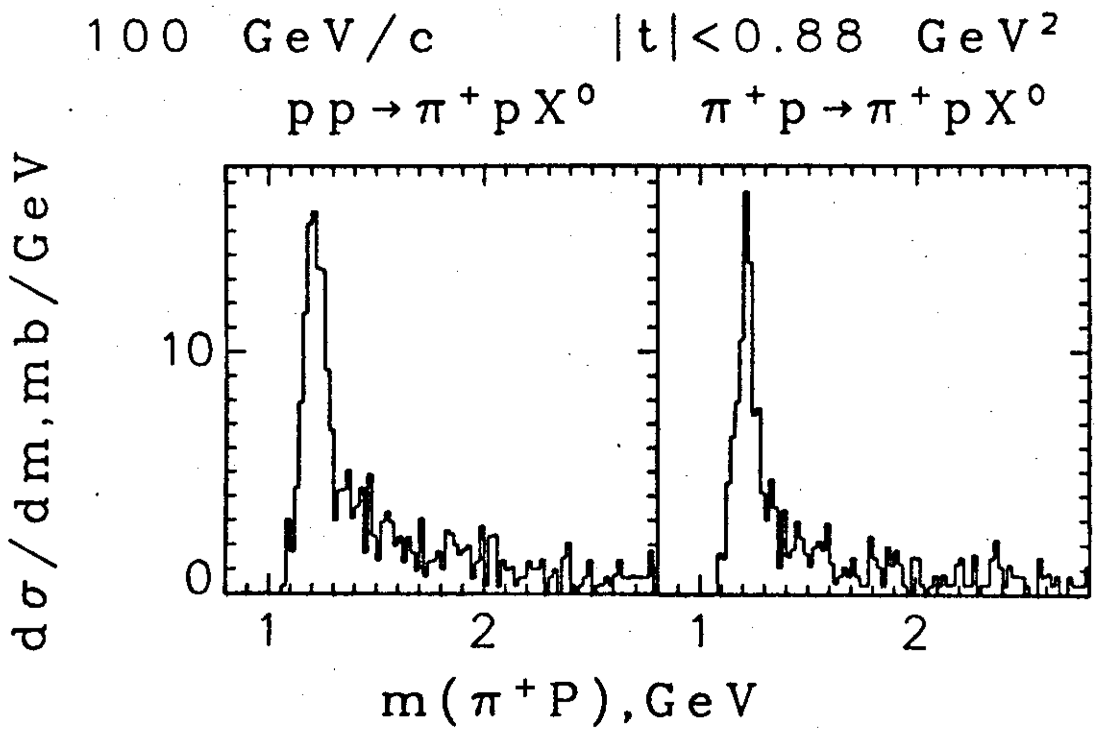

100 GeV/c
|t|<0.88 GeV²
pp→π⁺pX⁰
π⁺p→π⁺pX⁰
dσ/dm,mb/GeV
10
0
1
2
1
2
m(π⁺P),GeV

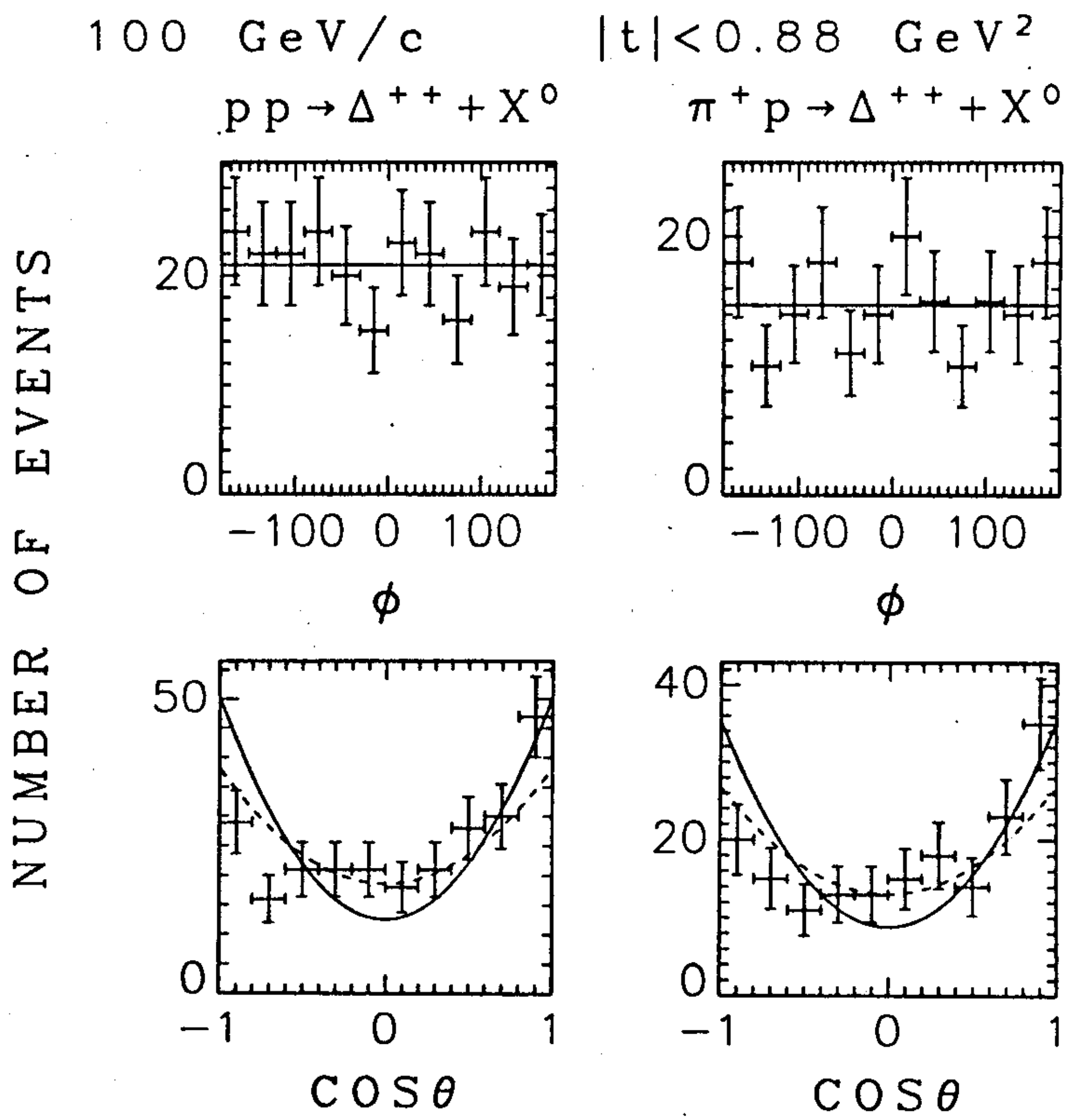

100 GeV/c
|t|<0.88 GeV²
pp → Δ⁺⁺ + X⁰
π⁺p → Δ⁺⁺ + X⁰
NUMBER OF EVENTS
0
20
0
20
−100 0 100
−100 0 100
φ
φ
0
50
0
20
40
−1 0 1
−1 0 1
COSθ
COSθ

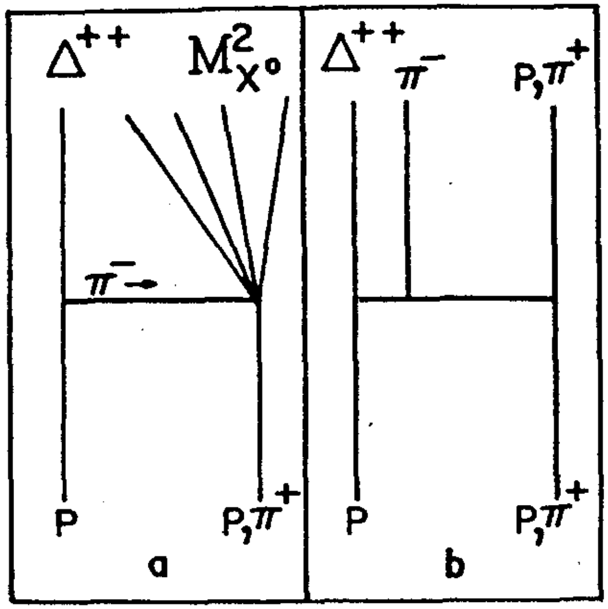

Δ++
M²X°
π⁻→
P
P,π+
a
Δ++
π⁻
P,π+
P
P,π+
b

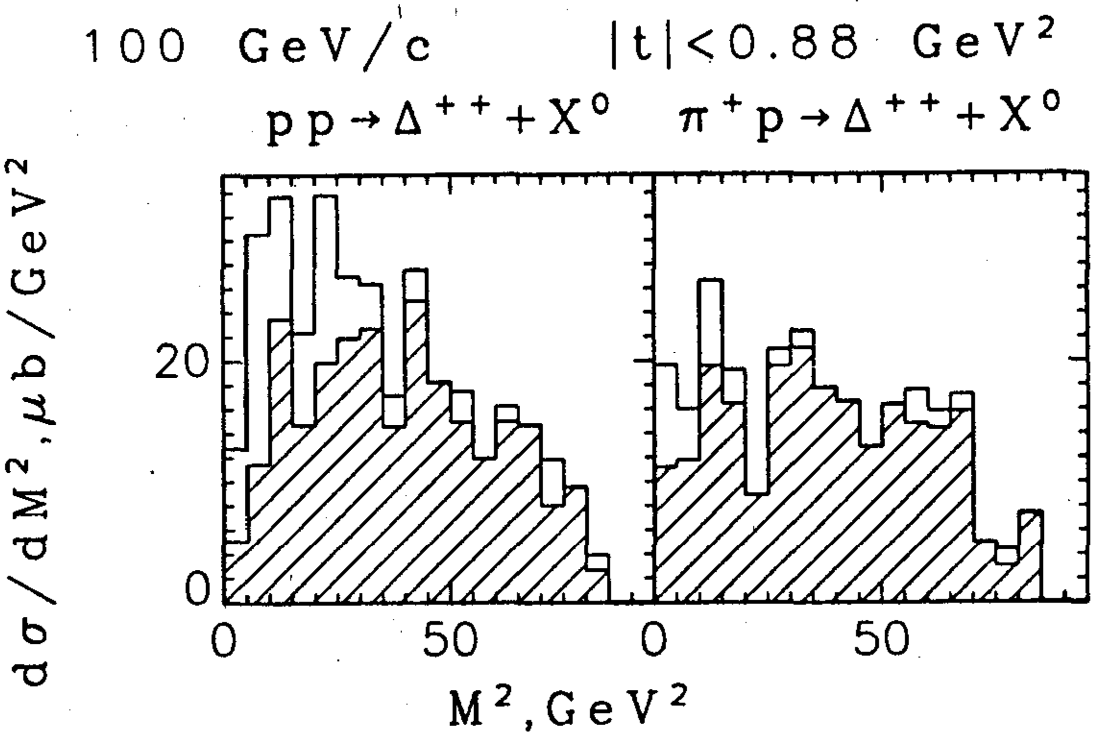

100 GeV/c
|t|<0.88 GeV²
pp → Δ⁺⁺ + X⁰
π⁺p → Δ⁺⁺ + X⁰
dσ/dM², μb/GeV²
20
0
0
50
0
50
M², GeV²

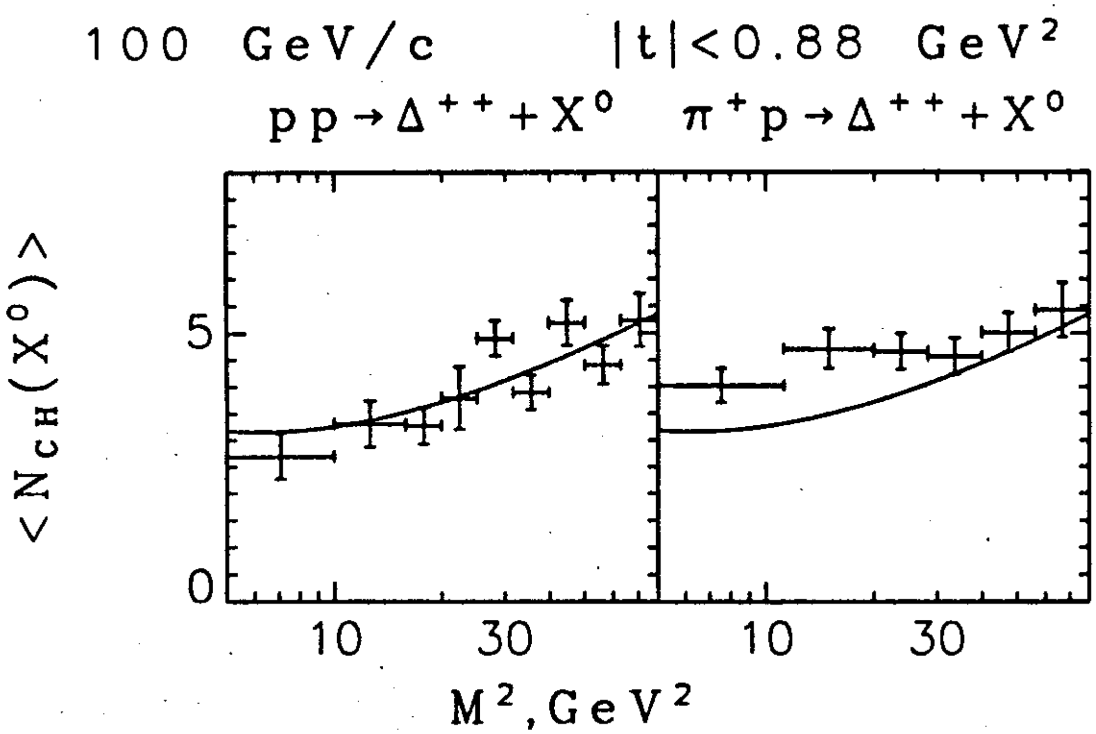
100 GeV/c
|t|<0.88 GeV²
pp→Δ⁺⁺+X⁰
π⁺p→Δ⁺⁺+X⁰
<NCH(X⁰)>
5
0
10
30
10
30
M², GeV²

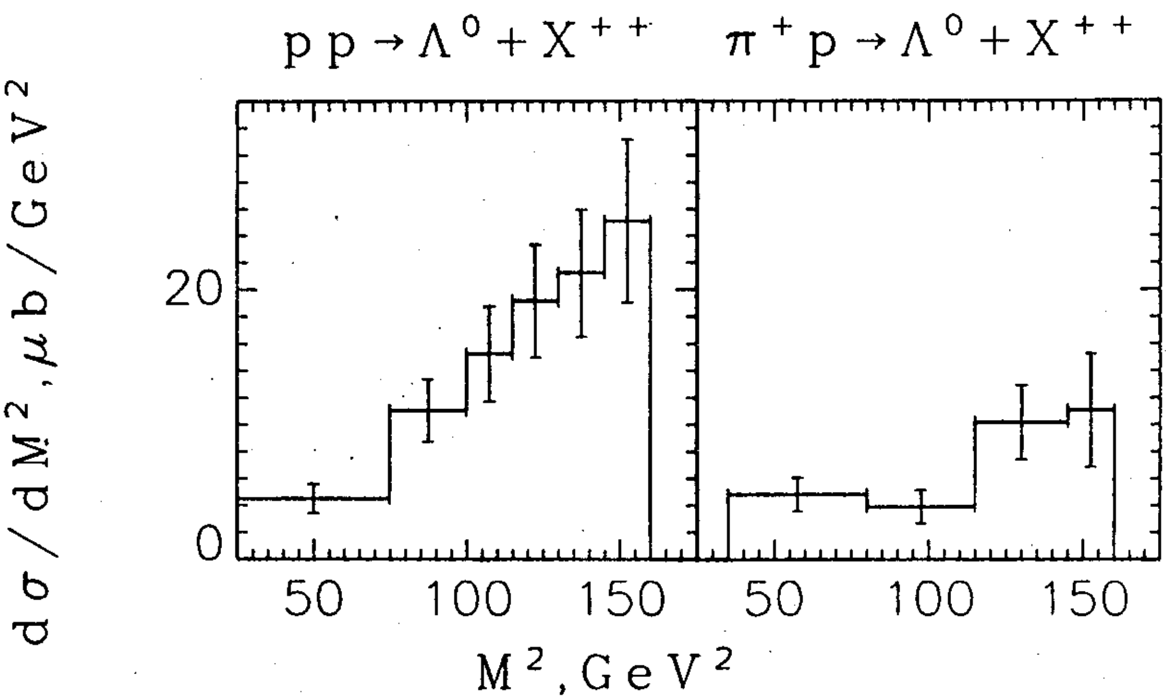

p p → Λ⁰ + X⁺⁺
π⁺ p → Λ⁰ + X⁺⁺
d σ / d M², μ b / G e V²
0
20
50
100
150
50
100
150
M², G e V²

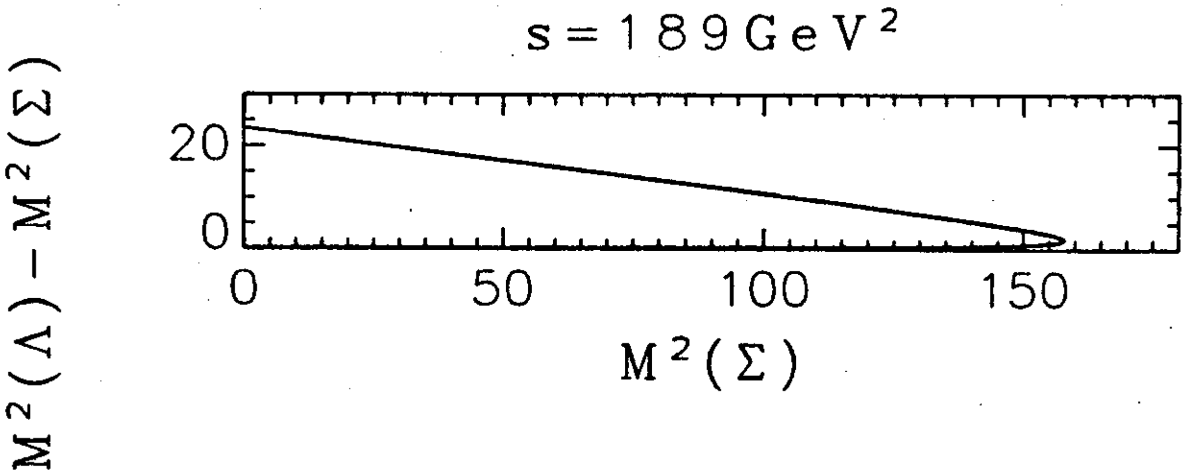

s = 189 GeV²
M²(Λ) − M²(Σ)
20
0
0
50
100
150
M²(Σ)

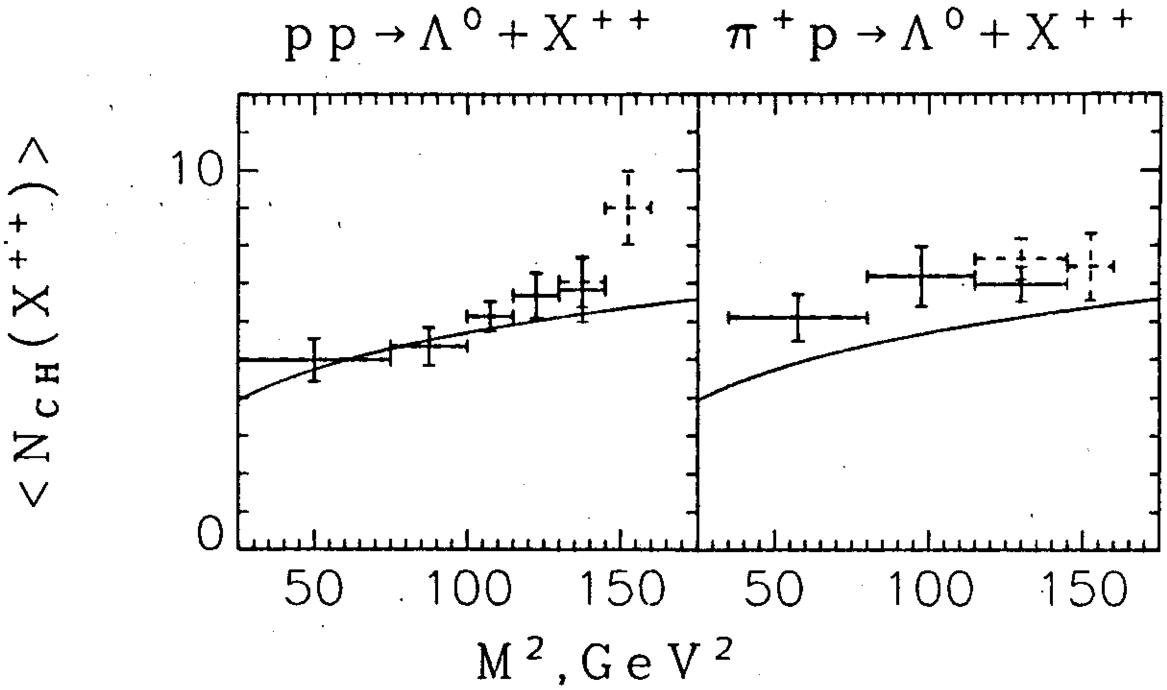

p p → Λ⁰ + X⁺⁺
π⁺ p → Λ⁰ + X⁺⁺
< N_CH (X⁺⁺) >
10
0
50
100
150
50
100
150
M², GeV²